A delay differential equation solver for MONOLIX & MLXPLORE

Raphaël Kuate, Marc Lavielle, Eric Blaudez, Kaelig Chatel, Jerome Marquet, Jean-François Si Abdallah

A delay differential equation solver for MONOLIX & MLXPLORE

Raphaël Kuate, Marc Lavielle, Eric Blaudez, Kaelig Chatel, Jerome Marquet, Jean-François Si Abdallah

RESEARCH REPORT
N° 8489
January 2014
Project-Teams Popix

ISSN 0249-6399 ISRN INRIA/RR--8489--FR+ENG

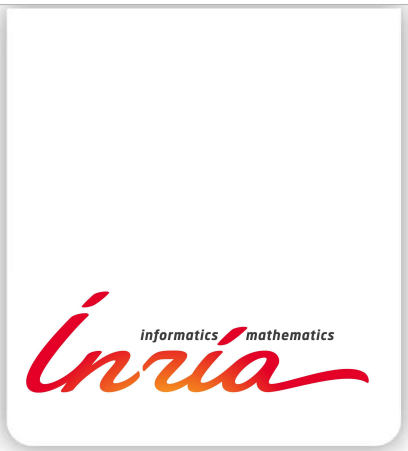

A delay differential equation solver for Monolix & MlxPlore

Raphaël Kuate*, Marc Lavielle†, Eric Blaudez‡, Kaelig Chatel§, Jerome Marquet¶, Jean-François Si Abdallah‖

Project-Teams Popix

Research Report n° 8489 — January 2014 — 19 pages

Abstract: We describe the implementation of a Delay differential Equation (DDE) solver in Monolix, a platform for population modeling of longitudinal data, and MlxPlore, a tool for the exploration of complex models. We use explicit Runge-Kutta schemes. Several examples for MlxPlore and Monolix are proposed.

Key-words: delay differential equations, solver, algorithm, Runge-Kutta formulas, modeling, pharmacokinetics, pharmacodynamics, Monolix, MlxPlore

* ✉: raphael.kuate@inria.fr
† ✉: marc.lavielle@inria.fr
‡ ✉: eric.blaudez@lixoft.net
§ ✉: kaelig.chatel@lixoft.net
¶ ✉: jerome.marquet@lixoft.net
‖ ✉: jean-francois.si_abdallah@lixoft.net

RESEARCH CENTRE
SACLAY – ÎLE-DE-FRANCE

1 rue Honoré d'Estienne d'Orves
Bâtiment Alan Turing
Campus de l'École Polytechnique
91120 Palaiseau

Résolution numérique d'équations différentielles avec retard dans Monolix & MlxPlore

Résumé : Ce document décrit l'implémentation d'un solveur d'équations différentielles avec retard (DDE) pour les logiciels Monolix et MlxPlore.

Mots-clés : équations différentielles avec retard, solveur, algorithmique, formules de Runge-Kutta, modélisation, pharmacocinétique, pharmacodynamique, Monolix, MlxPlore

1 Introduction

MONOLIX (MOdèles NOn LInéaires à effets miXtes) [2, 27, 16, 37] is a platform of reference for model-based drug development. It combines the most advanced algorithms with unique ease of use. Pharmacometricians of preclinical and clinical groups can rely on MONOLIX for population analysis and to model pharmacokinetic/pharmacodynamic (PK/PD) and other complex biochemical and physiological processes [29, 26, 39]. MONOLIX is an easy, fast and powerful tool for parameter estimation in non-linear mixed effect models, model diagnosis and assessment, and advanced graphical representation.

MLXPLORE [1] is a graphical and interactive software for the exploration and visualization of complex pharmacometric models. MLXPLORE also includes the ability to study the statistical variability of the models, and to model and study complex administrations designs. MLXPLORE is based on the Mlxtran model description language popularized by the MONOLIX software, therefore benefiting from the remarkable flexibility and power of Mlxtran to easily encode complex pharmacometric, PKPD and statistical models. MLXPLORE does not require MONOLIX, although they make for a powerful combination, enabling to use the same, human-readable model description, to finely explore the properties of the model on the one hand, and on the other hand use the same model for advanced parameter estimation in the context of population analysis and mixed effect statistics.

Modeling complex biological phenomenons with ordinary differential equations (ODEs) sometimes involves a large number of variables and parameters, which makes the analysis of these models cumbersome. Modeling such systems with delay differential equations (DDEs) helps to describe the important dynamics with fewer variables and parameters [44]. Another advantage of using a DDE model over an ODE model is that the parameters in the DDE model usually have a direct biological interpretation [4]. Thus, providing MONOLIX and MLXPLORE with a DDE solver is of a major importance.

Observing that the Taylor expansion of higher order of the solution of a DDE system needs derivatives of the delayed terms, we augment the DDE system being solved with the derivatives of the delayed terms. Then we apply classical explicit Runge-Kutta schemes on the new augmented system. We have implemented two variants of timestep: an adaptive timestep and a fixed timestep of which we propose its computation with respect to the CFL condition. We also propose an algorithm for the generation of the fixed time grid such that no interpolation of delayed terms be computed.

The document is organized as follows. In the second section we describe the implementations of the algorithms. Two variants of timestep are used: a fixed timestep and an adaptive timestep. In the fixed timestep case, a version uses the delayed solution, computed simultaneously during the simulation and a second version uses interpolated delayed solution. The numerical schemes implemented in the fixed timestep case are explicit Runge-Kutta formulas of order 2, 3 and 4. In the adaptive timestep version, the numerical schemes coded are Runge-Kutta embedded pairs [33, 19, 9, 43] of type 2(1), 3(2) and 4(3), using of course interpolated delayed solution. In the third section, we give some examples of numerical tests on DDEs, solved using MLXPLORE. In the fourth section, we present examples of estimation of parameters of DDE models, computed with MONOLIX.

2 Algorithms

The algorithms implemented use the well-known Runge-Kutta numerical schemes [3, 10, 11, 14, 8, 43, 45, 46].

2.1 Runge-Kutta schemes

ODEs Let Y be a time-dependent vector of real unknowns and let $\dot{Y}$ be the time derivative of Y. Let the vector $F(t, Y)$ be a function of Y and of the time t, and let Y_0 be the initial condition at the starting time t_0. The usual form of a differential equation of order 1 which can be found in PK/PD or biological [20, 34, 36, 42, 25] models writes:

$$\begin{cases} \dot{Y}(t) = F(t, Y), \quad t \in [t_0, T], \\ Y(t_0) = Y_0. \end{cases} \tag{2.1.1}$$

The numerical approximation of the solution of equation (2.1.1) using standard explicit Runge-Kutta numerical scheme is done as follows. Let $t_n \in [t_0, T]$ be a value of the time grid, and denote Y_n the value of Y at time t_n. Let $s, p \geq 1$ be two integers and let $h_n = t_{n+1} - t_n$ be the timestep. An explicit Runge-Kutta scheme of s stages and of order p writes:

$$\begin{cases} Y_{n+1} = Y_n + h_n \sum_{i=1}^{s} b_i K_i, \\ K_i = F\Big(t_n + c_i h_n, Y_n + \sum_{j=1}^{i-1} a_{i,j} K_j\Big), \quad i = 2, ..., s, \\ K_1 = F(t_n, Y_n), \end{cases} \tag{2.1.2}$$

where the coefficients $a_{ij}, b_i, c_i \in \mathbb{R}$ are obtained by solving a system of equations [12, 13] which results of an identification of (2.1.2) with the Taylor expansion of order p of Y, with respect to (2.1.1).

DDEs Many developments have been made [31, 5, 28, 41, 40, 7, 15, 6] on numerical methods for delay differential equations. We use standard explicit Runge-Kutta formulas, adapted to DDEs. For sake of simplicity, we describe the derivation of an explicit Runge-Kutta numerical scheme for DDEs, in the case $s = p = 2$.

Let N be a positive integer and $\tau \in \mathbb{R}_+^N$ be the vector of delays and denote $Y_{\tau_i} = Y(t - \tau_i)$. Let Y_0 be a function of the time t, and of $\tau_i, 1 \leq i \leq N$. The usual form of a delayed differential equation of order 1 which can be found in PK/PD or biological [4, 30, 44, 24] models writes:

$$\begin{cases} \dot{Y}(t) = F(t, Y, Y_{\tau_1}, ..., Y_{\tau_N}), & t \in [t_0, T], \\ Y(t) = Y_0(t, \tau), & t \leq t_0. \end{cases} \tag{2.1.3}$$

The Taylor expansion of order 2 of Y gives:

$$Y_{n+1} = Y_n + h_n \dot{Y}_n + \frac{1}{2} h_n^2 \ddot{Y}_n + \mathcal{O}(h_n^3). \tag{2.1.4}$$

Denote F_Y the matrix of the derivatives of F with respect to Y. The time derivative of Y of order 2, expressed in terms of F with respect to (2.1.3), writes:

$$\ddot{Y} = \dot{F} + F_Y F + \sum_{i=1}^{N} F_{Y_{\tau_i}} \dot{Y}_{\tau_i}. \tag{2.1.5}$$

If one does not neglect $\dot{Y}_{\tau_i}$, it appears from (2.1.5) that one needs $\dot{Y}_{\tau_i}$ in order to identify the coefficients of an explicit Runge-Kutta formula for the numerical approximation of (2.1.3). Thus, system (2.1.3) is augmented as follows:

$$\begin{cases} \dot{Y}(t) = F(t, Y, Y_{\tau_1}, ..., Y_{\tau_N}), & t \in [t_0, T], \\ \dot{Y}_{\tau_i}(t) = F(t - \tau_i, Y_{\tau_i}, Y_{\tau_1 + \tau_i}, ..., Y_{\tau_N + \tau_i}), & t \in [t_0, T], \quad 1 \leq i \leq N. \\ Y(t) = Y_0(t, \tau), & t \leq t_0. \end{cases} \tag{2.1.6}$$

Define $Z := \{Y, Y_{\tau_1}, ..., Y_{\tau_N}\}$, set $Z_0(t) = Y_0(t, \tau),\ t \leq t_0$, and define

$$F(t,Z) := \left\{ \begin{array}{c} F(t, Y, Y_{\tau_1}, ..., Y_{\tau_N}) \\ F(t-\tau_1, Y_{\tau_1}, Y_{\tau_1+\tau_1}, ..., Y_{\tau_N+\tau_1}) \\ F(t-\tau_2, Y_{\tau_2}, Y_{\tau_1+\tau_2}, ..., Y_{\tau_N+\tau_2}) \\ \vdots \\ F(t-\tau_N, Y_{\tau_N}, Y_{\tau_1+\tau_N}, ..., Y_{\tau_N+\tau_N}) \end{array} \right\}.$$

One has:

$$\left\{ \begin{array}{ll} \dot{Z}(t) = F(t,Z), & t \in [t_0, T], \\ Z(t) = Z_0(t), & t \leq t_0. \end{array} \right. \tag{2.1.7}$$

System (2.1.7) is used instead of (2.1.3) for the computations with standard Runge-Kutta formulas. Thus, an explicit Runge-Kutta scheme of s stages and of order p for the numerical approximation of (2.1.3) writes:

$$\left\{ \begin{array}{l} Z_{n+1} = Z_n + h_n \sum_{i=1}^{s} b_i K_i, \\ K_i = F\Big(t_n + c_i h_n, Z_n + \sum_{j=1}^{i-1} a_{i,j} K_j\Big), \quad i = 2, ..., s, \\ K_1 = F(t_n, Z_n), \end{array} \right. \tag{2.1.8}$$

where the coefficients $a_{ij}, b_i, c_i \in \mathbb{R}$ are obtained by solving a system of equations which results of an identification of (2.1.8) with the Taylor expansion of order p of Z, with respect to (2.1.7).

2.2 Solver features

2.2.1 Fixed timestep

The solver has a feature which uses a fixed timestep, with two sub-features. The first sub-feature uses cubic Hermite interpolation for the computation of delayed terms, since the solution and its time first order derivative are computed simultaneously. The second sub-features does not use interpolation. Let Ω be the discretization of the time interval. $\Omega = \{t_k,\ t_k \in [t_0, T]\}$ is computed such that:

$$\forall t_n \in \Omega,\ t_n - \tau_i \geq t_0 \Longrightarrow t_n - \tau_i \in \Omega,\ 1 \leq i \leq N. \tag{2.2.1}$$

The table T_Ω containing elements of Ω is returned with a table of numbers of the entries of T_Ω which contains $t_n - \tau_i, \forall t_n \in \Omega, 1 \leq i \leq N$. Thus for any $Y_n = Y(t_n)$ computed, one knows the delayed terms $Y(t_n - \tau_i)$ already computed, since statement (2.2.1) is always satisfied.

In the second sub-feature where the time grid contains delayed terms, the computation of T_Ω is done using Algorithm 1, for a given a timestep Δ_t.

Computation of the timestep In numerical simulation of time-dependent equations, numerical instabilities can occur, particularly for explicit numerical schemes [35, 21, 38, 47, 3, 32, 23]. Since the timestep Δ_t is fixed, one must compute Δ_t with respect to the Courant-Friedrichs-Lewy [17, 18] condition. Let $\#z$ be the size of Z and let $I_{\#z}$ be the identity matrix of the size of Z. The first order time derivative of Z is approached from (2.1.7) with the following:

$$\dot{Z} \approx F_Z Z,$$

of which an explicit numerical discretization writes:

$$Z_{n+1} \approx \Big[I_{\#z} + \Delta_{t_n}\{F_Z\}_n\Big] Z_n.$$

Algorithm 1 Time grid computation.

T_Ω inserts t_0, $t_1 \leftarrow T$, inserts t_1 into T_Ω in descending order.
while the biggest stepsize between t_1 and t_0 is greater than Δ_t **do**
  $t_j \leftarrow t_1$, $t_k \leftarrow t_1$
  while $t_j \geq t_0$ **do**
    for all $i, 1 \leq i \leq N$ **do**
      $t_i \leftarrow t_j - \tau_i$
      if $t_i \geq t_0$ **then**
        put a flag on t_i
        inserts t_i into T_Ω in descending order.
      end if
    end for
    $t_j \leftarrow$ the next entry of T_Ω with a flag, after t_k in descending order
    in T_Ω, remove the flag on t_j
    $t_k \leftarrow t_j$
  end while
  $t_1 \leftarrow t_1 - \Delta_t$
  if $t_1 \geq t_0$ **then**
    inserts t_1 into T_Ω in descending order.
  end if
end while
rearrange T_Ω in ascending order

The timestep Δ_t is then computed such that (2.2.2) be satisfied.

$$\left\| \left[I_{\#z} + \Delta_t F_Z \right] Z \right\| = CFL < 1. \tag{2.2.2}$$

Let $z_i, 1 \leq i \leq \#z$, be the i-th entry of Z. The timestep Δ_t is obtained from (2.2.2) with

$$z_i = \frac{1}{\sqrt{\#z}},\ 1 \leq i \leq \#z, \quad i.e.,\ \|Z\| = 1.$$

Let $Z^i, 1 \leq i \leq \#z$, be the vector of the size $\#z$ containing z_i at the i-th entry and zeros elsewhere. Since F_Z may be time dependent, let F_Z^k be its value for $t = t_k$. The i-th column of F_Z^k is obtained by evaluating the following expression

$$F_Z^{i,k} = \frac{F(t_k, Z + \alpha Z^i) - F(t_k, Z)}{\alpha}, \quad 1 \leq i \leq \#z, \quad O < \alpha \ll 1.$$

For each t_k chosen, one obtains a value Δ_{t_k} of Δ_t from (2.2.2). The time interval $[t_0, T]$ is uniformly meshed and

$$t_k = t_0 + \frac{k}{\#nk}(T - t_0),\ 0 \leq k \leq \#nk, \quad \#nk < 20.$$

The timestep Δ_t is taken as the minimum of the Δ_{t_k}'s. However, one checks if F_Z is not time dependent by comparing $F(t_0, Z)$ with $F(t_1, Z)$, and the computations are stopped if $F(t_0, Z) \equiv F(t_1, Z)$.

Coefficients of the Runge-Kutta formulas In the fixed timestep feature of the solver, the numerical schemes implemented are explicit Runge-Kutta formulas of order 2, 3 and 4:

$$\begin{cases} Z_{n+1} = Z_n + h_n \sum_{i=1}^{s} b_i K_i, \\ K_i = F\Big(t_n + c_i h_n, Z_n + \sum_{j=1}^{i-1} a_{i,j} K_j\Big), \quad i = 2, ..., s, \\ K_1 = F(t_n, Z_n). \end{cases}$$

The coefficients $a_{i,j}, b_i$ and c_i can be stored in a table called Butcher tableau defined in table 1.

c_2	$a_{2,1}$				
$\vdots$	$\vdots$	$\ddots$			
c_{s-1}	$a_{s-1,1}$	$a_{s-1,2}$	$\dots$		
c_s	$a_{s,1}$	$a_{s,2}$	$\dots$	$a_{s,s-1}$	
	b_1	b_2	$\dots$	b_{s-1}	b_s

Table 1: The Butcher tableau of the Runge-Kutta coefficients.

The coefficients used are given in the Butcher tableaux, table 2, and can be found in [12, 11, 10].

Order 2:

$\frac{1}{2}$	$\frac{1}{2}$	
	$\frac{1}{2}$	$\frac{1}{2}$

Order 3:

$\frac{1}{2}$	$\frac{1}{2}$		
$\frac{1}{2}$	-1	2	
	$\frac{1}{6}$	$\frac{2}{3}$	$\frac{1}{6}$

Order 4:

$\frac{1}{2}$	$\frac{1}{2}$			
$\frac{1}{2}$	0	$\frac{1}{2}$		
1	0	0	1	
	$\frac{1}{6}$	$\frac{1}{3}$	$\frac{1}{3}$	$\frac{1}{6}$

Table 2: Some Butcher tableaux of Runge-Kutta explicit scheme of order 2, 3 and 4.

2.2.2 Adaptive timestep

The model considered is the augmented system (2.1.7). In an adaptive timestep method, the timestep is computed such that the method of order p be more accurate than an embedded method of order $p' < p$. Generally, one choses $p' = p - 1$. In a step n, the local error $E_n = \|Z_n - Z'_n\|$ between the approximation Z of order p and the approximation Z' of order p' is used to validate or not the step and to compute the timestep for the next step.

$$Z_{n+1} = Z_n + h_n \sum_{i=1}^{s} b_i K_i, \quad Z'_{n+1} = Z'_n + h_n \sum_{i=1}^{s} b'_i K_i.$$

The coefficients of the Runge-Kutta formula for these two approximations are computed such that the coefficients $a_{i,j}$, and c_i (2.1.8) of the two approximations be the same. Some embedded

pairs also use the FSAL (first same as the last) strategy *i.e.,* when a step is accepted, the last coefficient K_s becomes the first coefficient K_1 of the next step, which reduces the method to a $s-1$ stage method. Many strategies [14, 41, 43, 22, 45, 46] have been developed for the computation of adaptive timesteps. The strategy used is a standard formula described in [14, 45]. Given a tolerance TOL the algorithm computes the next timestep h_{n+1} with the following formula:

$$h_{n+1} = \theta\, h_n \left(\frac{TOL}{E_n}\right)^{\frac{1}{p}}, \quad \theta \in (0,1).$$

The next stepsize h_{n+1} is accepted if $TOL \geq E_n$. If $TOL < E_n$ the current step n is rejected and recomputed again with $h_n \leftarrow h_{n+1}$.

The first timestep h_1 is computed [14] as

$$h_1 = \left(\frac{TOL}{\max\left\{\|F(t_0, Z_0)\|, 10^{-p}\right\}}\right)^{\frac{1}{p}}.$$

The Butcher tableau for Runge-Kutta embedded pairs is defined in table 3.

c_2	$a_{2,1}$				
$\vdots$	$\vdots$	$\ddots$			
c_{s-1}	$a_{s-1,1}$	$a_{s-1,2}$	$\dots$		
c_s	$a_{s,1}$	$a_{s,2}$	$\dots$	$a_{s,s-1}$	
	b_1	b_2	$\dots$	b_{s-1}	0
	b'_1	b'_2	$\dots$	b'_{s-1}	b'_s

Table 3: The Butcher tableau of coefficients of the Runge-Kutta embedded pairs.

Runge-Kutta coefficients In the adaptive timestep feature of the solver, the numerical schemes implemented are Runge-Kutta embedded FSAL pairs of M. Sofroniou and G. Spaletta [43], of type 2(1), 3(2) and 4(3). The Butcher tableaux are given in tables 4 and 5.

Type 2(1):

1	1		
1	$\frac{1}{2}$	$\frac{1}{2}$	
	$\frac{1}{2}$	$\frac{1}{2}$	0
	1	$-\frac{1}{6}$	$\frac{1}{6}$

Type 3(2):

$\frac{1}{2}$	$\frac{1}{2}$			
1	-1	2		
1	$\frac{1}{6}$	$\frac{2}{3}$	$\frac{1}{6}$	
	$\frac{1}{6}$	$\frac{2}{3}$	$\frac{1}{6}$	0
	$\frac{22-\sqrt{82}}{72}$	$\frac{14+\sqrt{82}}{36}$	$\frac{-4+\sqrt{82}}{144}$	$\frac{16-\sqrt{82}}{48}$

Table 4: The Butcher tableaux of Runge-Kutta FSAL pairs of M. Sofroniou and G. Spaletta [43], of types 2(1) and 3(2).

Type 4(3):

$\frac{2}{5}$	$\frac{2}{5}$				
$\frac{3}{5}$	$-\frac{3}{20}$	$\frac{2}{4}$			
1	$\frac{19}{44}$	$-\frac{15}{44}$	$\frac{10}{11}$		
1	$\frac{11}{72}$	$\frac{25}{72}$	$\frac{25}{72}$	$\frac{11}{72}$	
0	$\frac{11}{72}$	$\frac{25}{72}$	$\frac{25}{72}$	$\frac{11}{72}$	0
	$\frac{1251515}{8970912}$	$\frac{3710105}{8970912}$	$\frac{2519695}{8970912}$	$\frac{61105}{8970912}$	$\frac{119041}{757576}$

Table 5: The Butcher tableau of Runge-Kutta FSAL pairs of M. Sofroniou and G. Spaletta [43], of type 4(3).

3 Simulation of DDEs using MLXPLORE

Example 3.1

The model solved is the SEIR epidemic model of Genik & van den Driessche, example 4.4.1 of

[40] defined by:

$$\begin{cases} N(t) = & S(t) + E(t) + I(t) + R(t) \\ \dot{S}(t) = & A(t) - S(t) - \lambda \dfrac{S(t)I(t)}{N(t)} + \gamma I(t-\tau)\exp(-d\tau), \\ \dot{E}(t) = & \lambda \dfrac{S(t)I(t)}{N(t)} - dE(t) - \lambda \dfrac{S(t-\omega)I(t-\omega)\exp(-d\omega)}{N(t-\omega)}, \\ \dot{I}(t) = & -(\gamma + \epsilon + d)I(t) + \lambda \dfrac{S(t-\omega)I(t-\omega)\exp(-d\omega)}{N(t-\omega)}, \\ \dot{R}(t) = & \gamma I(t) - dR(t) - \gamma I(t-\tau)\exp(-d\tau), \qquad t \in [0, 350]. \end{cases} \tag{3.1.1}$$

The history is given by

$$S(t) = 15,\ E(t) = 0,\ I(t) = 2,\ R(t) = 3,\ t \leq 0.$$

The parameters are

$$A = 0.33,\ d = 0.006,\ \lambda = 0.308,\ \gamma = 0.04,\ \epsilon = 0.06, \tau = 42,\ \omega = 0.15. \tag{3.1.2}$$

The MlxPlore script of this example is given in the section below

MlxPlore script

```
<MODEL>
[PREDICTION]
input = {A,d,lambda,gamma,epsilon,omega,tau}
EQUATION:
t0 = 0
S_0 = 15
E_0 = 0
I_0 = 2
R_0 = 3
N = S + E + I + R

ddt_S = A - d*S -lambda*S*I/N +gamma*delay(I,tau)*exp(-d*tau)
ddt_E =  -  lambda*delay(S,omega)*delay(I,omega)*exp(-d*omega)/(delay(I,omega)
              + delay(S,omega) + delay(E,omega) + delay(R,omega))
                + lambda*S*I/N - d*E
ddt_I = - (gamma + epsilon + d)*I
           + lambda*delay(S,omega)*delay(I,omega)*exp(-d*omega)/(delay(I,omega)
           + delay(S,omega)  + delay(E,omega) + delay(R,omega))
ddt_R = gamma*I - d*R  - gamma*delay(I,tau)*exp(-d*tau)

<PARAMETER>
A = 0.33
d = 0.006
lambda = 0.308
gamma = 0.04
epsilon = 0.06
tau = 42
omega = 0.15
<OUTPUT>
list = {S,E,I,R}
grid = 0:1:350
```

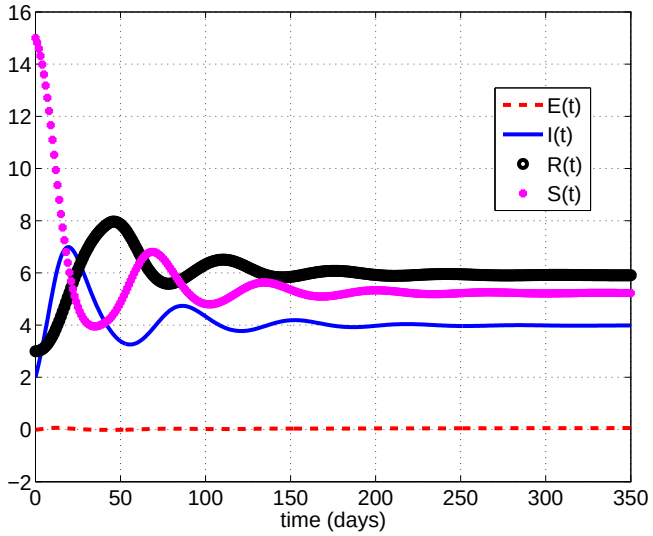

Figure 1: The SEIR epidemic model of Genik & van den Driessche, example 4.4.1 of [40].

Example 3.2

The model solved is the Interleukin-2: model studied by Baker *et al.* in [4] and defined by:

$$\begin{cases} \dot{I}_2(t) = & -\alpha_{I_2} I_2(t) - n_{I_2} b_{TI_2} \dfrac{I_2(t)}{I_2(t)/I_2^* + 1} T_A(t), \\ \dot{T}_A(t) = & \rho b_{TI_2} \dfrac{I_2(t-\tau_D)}{I_2(t-\tau_D)/I_2^* + 1} T_A(t-\tau_D) \\ & -b_{TI_2} \dfrac{I_2(t-\tau_S)}{I_2(t-\tau_S)/I_2^* + 1} T_A(t-\tau_S) - \alpha_{AR} T_A(t), \\ \dot{T}_D(t) = & b_{TI_2} \dfrac{I_2(t-\tau_S)}{I_2(t-\tau_S)/I_2^* + 1} T_A(t-\tau_S) \\ & -b_{TI_2} \dfrac{I_2(t-\tau_D)}{I_2(t-\tau_D)/I_2^* + 1} T_A(t-\tau_D), \\ \dot{T}_R(t) = & \alpha_{AR} T_A(t) - \alpha_R T_R(t), \qquad t \in [0, 100]. \end{cases} \tag{3.2.1}$$

The parameters of model (3.2.1) are

$$\begin{array}{c} \alpha_{I_2} = 0,\ \alpha_R = 1.5 \cdot 10^{-2},\ \alpha_{AR} = 6.6 \cdot 10^{-2},\ n_{I_2} = 4755, \\ b_{TI_2} = 1.8 \cdot 10^{-11},\ I_2^* = 6 \cdot 10^{10},\ \tau_D = 6.6,\ \tau_S = 10,\ \rho = 2. \end{array} \tag{3.2.2}$$

The model (3.2.1) is compared in [4] with an ODE model of the same phenomenon, defined as follows:

$$\begin{cases} \dot{I}_2(t) = & -\alpha_{I_2} I_2(t) - n_{I_2} b_{TI_2} \dfrac{I_2(t)}{I_2(t)/I_2^* + 1} T_A(t), \\ \dot{T}_A(t) = & \rho b_D T_D(t) - b_{TI_2} \dfrac{I_2(t)}{I_2(t)/I_2^* + 1} T_A(t) - \alpha_{AR} T_A(t), \\ \dot{T}_D(t) = & b_{TI_2} \dfrac{I_2(t)}{I_2(t)/I_2^* + 1} T_A(t) - b_D T_D(t), \\ \dot{T}_R(t) = & \alpha_{AR} T_A(t) - \alpha_R T_R(t), \qquad t \in [0, 100]. \end{cases} \tag{3.2.3}$$

The parameters of model (3.2.3) are

$$\alpha_{I_2} = 0,\ \alpha_R = 3.5 \cdot 10^{-2},\ \alpha_{AR} = 0.02,\ n_{I_2} = 4755,$$
$$b_{TI_2} = 1.0 \cdot 10^{-11},\ I_2^* = 6 \cdot 10^{10},\ b_D = 1/8,\ \rho = 2.$$

The history of models (3.2.1) and (3.2.3) is given by

$$I_2(t) = 2 \cdot 10^{10},\ T_A(t) = 3.8 \cdot 10^5,\ T_D(t) = 0,\ T_R(t) = 1.2 \cdot 10^5,\ t \leq 0.$$

The MlxPlore script of the dde model of this example is given in the section below

MlxPlore script

```
<MODEL>
[PREDICTION]
input = {alphaI2,alphaR,alphaAR,nI2,bTI2,starI2,tauD,tauS,rho}

EQUATION:
t0 = 0
I2_0 = 2e10
TA_0 = 3.8e5
TD_0 = 0
TR_0 = 1.2e5

ddt_I2 = - alphaI2*I2 - nI2*bTI2*I2*TA/(I2/starI2 + 1)
ddt_TA  = rho*bTI2*delay(I2,tauD)*delay(TA,tauD)/(delay(I2,tauD)/starI2 + 1)
                - bTI2* delay(I2,tauS)*delay(TA,tauS)/(delay(I2,tauS)/starI2 + 1)
               - alphaAR*TA
ddt_TD  =  bTI2 *delay(I2,tauS)*delay(TA,tauS)/(delay(I2,tauS)/starI2  + 1)
                - bTI2 *delay(I2,tauD)*delay(TA,tauD)/(delay(I2,tauD)/starI2 + 1 )
ddt_TR  = alphaAR*TA - alphaR*TR

TV = TA + TD + TR

<PARAMETER>
alphaI2 = 0
alphaR = 1.5e-2
alphaAR = 6.6e-2
nI2 = 4755
bTI2 = 1.8e-11
starI2 = 6e10
tauD = 6.6
tauS = 10
rho = 2
<OUTPUT>
list = {TV}
grid = 0:1:100
```

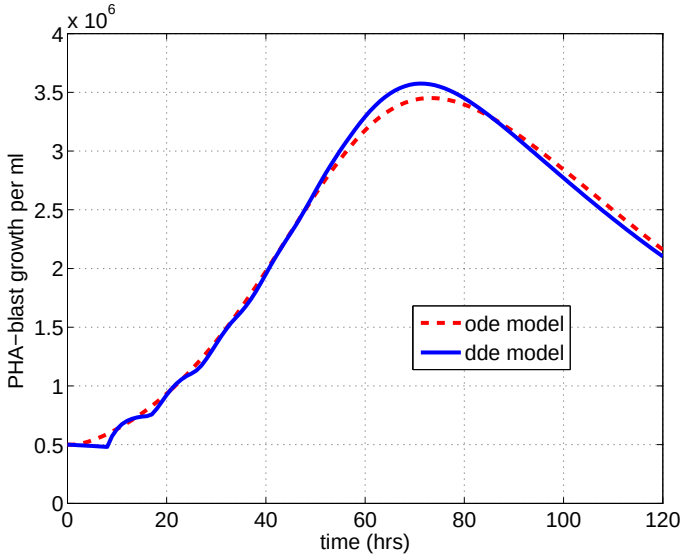

Figure 2: The Interleukin-2: model studied by Baker *et al.* in [4]

Example 3.3

The model solved is the PKPD model for unperturbed and perturbed arthritis development of Koch *et al.* [24] defined by:

$$\begin{cases} \dot{G}(t) = & k_3 - \Big(\sigma_1 \exp\left(-\sigma_2 c(t)\right) + \sigma_3\Big) c(t) G(t) - \dfrac{k_1}{k_2}\Big(1 - \exp\left(-k_2 t\right)\Big) G(t), \\ \dot{I}(t) = & k_4 G(t) - k_4 G(t-\tau), \\ \dot{D}(t) = & k_4 G(t-\tau) - k_5 D(t), \end{cases} \qquad t \in [0, 35].$$

The history is given by

$$G(t) = a \exp(bs),\ I(t) = I_0,\ D(t) = 0,\ t \leq 0.$$

The parameters are

$$a = 1,\ b = 0.5,\ k_1 = 0.183,\ k_2 = 0.092,\ k_3 = 5,\ k_4 = 0.064,\ k_5 = 0.016,\ \tau = 11.2.$$

The parameter $c(t)$ is given by a PK data *dose* of a standard linear 2-compartment i.v. model. The equation used in [24] is

$$c(t) = dose\Big(A_{iv} \exp(-\alpha t) + B_{iv} \exp(-\beta t)\Big).$$

However, $c(t)$ can be fitted with MLXPLORE, knowing the volumes V_1, V_2 of the compartments, the parameters α, β, CL, the *dose* (amount in Mlxtran) and the administration times of the PK model. The MLXPLORE script of this example is given in section the below

MLXPLORE script

```
<MODEL>
[PREDICTION]
```

```
input = {a,b,alpha,beta,sigma1,sigma2,sigma3, k1, k2, k3,k4,k5,tau,CL,V1,V2}

EQUATION:
t0 = 0
I_0 = 2.52
D_0 = 0
G_0 = a*exp(b*t)

K12 = alpha*beta*V2/CL
K21 = alpha*beta*V1/CL
C = pkmodel(k12=K12,k21=K21,V=V1,Cl=CL)

ddt_G = k3  - (sigma1*exp(- sigma2*C) + sigma3)*C*G - k1*(1- exp(- k2*t))*G/k2
ddt_I = k4*G - k4*delay(G,tau)
ddt_D  =  - k5*D + k4*delay(G,tau)


<DESIGN>
[ADMINISTRATION]
adm1 = {time = 1, amount = 10}
adm2 = {time = 8, amount = 10}
adm3 = {time = 15, amount = 10}
[TREATMENT]
trt1 = {adm1, adm2, adm3}
<PARAMETER>
CL = 0.0029
V1 = 0.0265
V2 = 0.0270
alpha = 0.2256
beta = 0.0065
a = 1
b = 0.5
sigma1 = 0.154
sigma2 = 0.065
sigma3 = 0.003
k1 = 0.183
k2 = 0.092
k3 = 5
k4 = 0.064
k5 = 0.016
tau = 11.2
<OUTPUT>
list = {G,I,D}
grid = 0:1:35
```

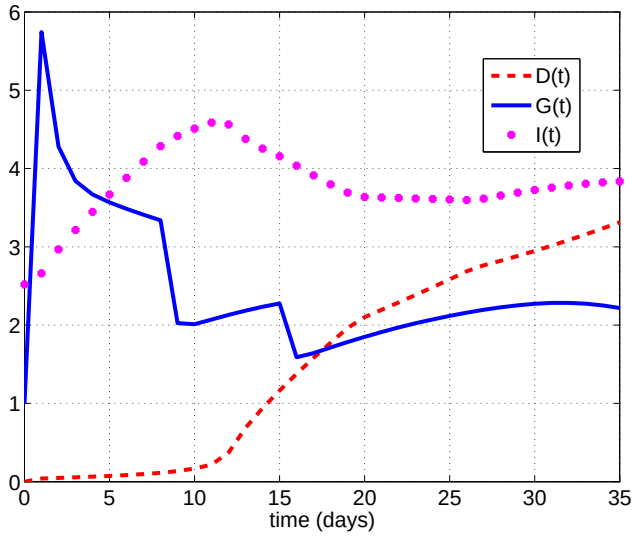

Figure 3: The PKPD model for unperturbed and perturbed arthritis development of Koch *et al.* [24], Experiment A with the dosing schedules: 10 mg/kg on day 1, 8, 15.

4 Estimation of parameters of DDEs using MONOLIX

4.1 Example 3.1

The data used for the estimations of parameters $A, \lambda, \gamma, \epsilon, \tau, d$ of model (3.1.1) are simulated with MLXPLORE, using the model with values of the parameters given in (3.1.2), of which a random noise has been added to the parameter d with a variance omega_d = 1.2.

A similar example can be found in the MONOLIX demos folder at
lixoft/monolix/monolix430/demos/dde/seir_projet.mlxtran

```
************************************************************************
*      ex4p4p1dde-2_projet.mlxtran
*      January 14, 2014 at 15:45:09
*      Monolix version: 4.3.0
************************************************************************
Estimation of the population parameters

                parameter
A             :     0.332
lambda        :     0.309
gamma         :    0.0399
epsilon       :    0.0602
d             :    0.0068
tau           :      42.1

omega_A       :    0.0118
omega_lambda  :   0.00428
omega_gamma   :     0.013
omega_epsilon :    0.0267
```

```
omega_d       :    0.811
omega_tau     :  0.00235
```

4.2 Example 3.2

The data used for the estimations of parameters τ_D, τ_S of model (3.2.1) are simulated with MlxPlore, using the model with values of the parameters given in (3.2.2).

A similar example can be found in the Monolix demos folder at
lixoft/monolix/monolix430/demos/dde/arthritis_projet.mlxtran

```
****************************************************************
*      Il2_projet.mlxtran
*      January 14, 2014 at 09:02:42
*      Monolix version: 4.3.0
****************************************************************
Estimation of the population parameters

             parameter
tauD       :      6.73
tauS       :      9.65

omega_tauD :  0.000115
omega_tauS :  0.000237
```

Contents

References

[1] MlxPlore *A software for model exploration and visualization.* http://www.lixoft.eu/products/mlxplore/mlxplore-documentation/.

[2] Monolix *A software for the analysis of nonlinear mixed effects models.* http://www.lixoft.eu/products/monolix/documentation/.

[3] Christopher TH Baker and Christopher AH Paul. Computing stability regions-Runge-Kutta methods for delay differential equations. *IMA Journal of Numerical Analysis*, 14(3):347–362, 1994.

[4] C.T.H. Baker, G.A. Bocharov, and C.A.H. Paul. Mathematical modelling of the interleukin-2 T-cell system: A comparative study of approaches based on ordinary and delay differential equations. *Journal of Theoretical Medicine*, 1(2):117–128, 1997.

[5] C.T.H. Baker, C.A.H. Paul, and D.R. Willé. Issues in the numerical solution of evolutionary delay differential equations. *Advances in Computational Mathematics*, 3(1):171–196, 1995.

[6] Robert J. Bauer, Gary Mo, and Wojciech Krzyzanski. Solving delay differential equations in S-ADAPT by method of steps. *Computer Methods and Programs in Biomedicine*, 111(3):715 – 734, 2013.

[7] Alfredo Bellen and Marino Zennaro. *Numerical methods for delay differential equations*. Oxford University Press, 2003.

[8] G. Vanden Berghe, H. De Meyer, M. Van Daele, and T. Van Hecke. Exponentially-fitted explicit Runge-Kutta methods. *Computer Physics Communications*, 123(1-3):7 – 15, 1999.

[9] P. Bogacki and L.F. Shampine. A 3(2) pair of Runge-Kutta formulas. *Applied Mathematics Letters*, 2(4):321 – 325, 1989.

[10] J. C. Butcher. A history of Runge-Kutta methods. *Appl. Numer. Math.*, 20(3):247–260, March 1996.

[11] J. C. Butcher and G. Wanner. Runge-Kutta methods: Some historical notes. *Appl. Numer. Math.*, 22(1-3):113–151, November 1996.

[12] John C Butcher. Coefficients for the study of Runge-Kutta integration processes. *J. Austral. Math. Soc*, 3:185–201, 1963.

[13] John C Butcher. On the attainable order of Runge-Kutta methods. *Math. Comp*, 19(408-417):2, 1965.

[14] M. Calvo, D.J. Higham, J.I. Montijano, and L. Ráindez. Stepsize selection for tolerance proportionality in explicit Runge-Kutta codes. *Advances in Computational Mathematics*, 7(3):361–382, 1997.

[15] Rodrigo Castro, Ernesto Kofman, and François E. Cellier. Quantization-based integration methods for delay-differential equations. *Simulation Modelling Practice and Theory*, 19(1):314 – 336, 2011. Modeling and Performance Analysis of Networking and Collaborative Systems.

[16] PhylindaL.S. Chan, Philippe Jacqmin, Marc Lavielle, Lynn McFadyen, and Barry Weatherley. The use of the SAEM algorithm in MONOLIX software for estimation of population pharmacokinetic-pharmacodynamic-viral dynamics parameters of maraviroc in asymptomatic HIV subjects. *Journal of Pharmacokinetics and Pharmacodynamics*, 38(1):41–61, 2011.

[17] R. Courant, K. Friedrichs, and H. Lewy. Über die partiellen differenzengleichungen der mathematischen physik. *Mathematische Annalen*, 100(1):32–74, 1928.

[18] R. Courant, K. Friedrichs, and H. Lewy. On the partial difference equations of mathematical physics. *IBM J. Res. Dev.*, 11(2):215–234, March 1967.

[19] J.R. Dormand and P.J. Prince. Runge-Kutta triples. *Computers & Mathematics with Applications*, 12(9, Part A):1007 – 1017, 1986.

[20] Johan L. Gabrielsson and Daniel L. Weiner. Methodology for pharmacokinetic/pharmacodynamic data analysis. *Pharmaceutical Science & Technology Today*, 2(6):244 – 252, 1999.

[21] Gopal K. Gupta, Ron Sacks-Davis, and Peter E. Tescher. A review of recent developments in solving ODEs. *ACM Comput. Surv.*, 17(1):5–47, March 1985.

[22] Alan C. Hindmarsh, Peter N. Brown, Keith E. Grant, Steven L. Lee, Radu Serban, Dan E. Shumaker, and Carol S. Woodward. Sundials: Suite of nonlinear and differential/algebraic equation solvers. *ACM Trans. Math. Softw.*, 31(3):363–396, September 2005.

[23] Z. Kalogiratou, Th. Monovasilis, G. Psihoyios, and T.E. Simos. Runge-Kutta type methods with special properties for the numerical integration of ordinary differential equations. *Physics Reports*, (0), 2013.

[24] Gilbert Koch, Thomas Wagner, Christine Plater-Zyberk, Gezim Lahu, and Johannes Schropp. Multi-response model for rheumatoid arthritis based on delay differential equations in collagen-induced arthritic mice treated with an anti-GM-CSF antibody. *Journal of Pharmacokinetics and Pharmacodynamics*, 39(1):55–65, 2012.

[25] Wojciech Krzyzanski and JuanJose Perez Ruixo. Lifespan based indirect response models. *Journal of Pharmacokinetics and Pharmacodynamics*, 39(1):109–123, 2012.

[26] Marc Lavielle and Cyprien Mbogning. An improved SAEM algorithm for maximum likelihood estimation in mixtures of non linear mixed effects models. *Statistics and Computing*, pages 1–15, 2013.

[27] Marc Lavielle and France Mentré. Estimation of population pharmacokinetic parameters of saquinavir in HIV patients with the MONOLIX software. *Journal of Pharmacokinetics and Pharmacodynamics*, 34(2):229–249, 2007.

[28] Tatyana Luzyanina, Koen Engelborghs, Kurt Lust, and Dirk Roose. Computation, continuation and bifurcation analysis of periodic solutions of delay differential equations. *International Journal of Bifurcation and Chaos*, 07(11):2547–2560, 1997.

[29] David Makowski and Marc Lavielle. Using SAEM to estimate parameters of models of response to applied fertilizer. *Journal of Agricultural, Biological, and Environmental Statistics*, 11(1):45–60, 2006.

[30] Alexander Y Mitrophanov, Gordon Churchward, and Mark Borodovsky. Control of streptococcus pyogenes virulence: Modeling of the CovR/S signal transduction system. *Journal of theoretical biology*, 246(1):113–128, 2007.

[31] Christopher A.H. Paul. Developing a delay differential equation solver. *Applied Numerical Mathematics*, 9(3-5):403 – 414, 1992.

[32] Linda R. Petzold, Laurent O. Jay, and Jeng Yen. Numerical solution of highly oscillatory ordinary differential equations. *Acta Numerica*, 6:437–483, 1 1997.

[33] PJ Prince and JR Dormand. High order embedded Runge-Kutta formulae. *Journal of Computational and Applied Mathematics*, 7(1):67–75, 1981.

[34] José Pérez-Urizar, Vinicio Granados-Soto, Francisco J Flores-Murrieta, and Gilberto Castañeda-Hernández. Pharmacokinetic-pharmacodynamic modeling: Why? *Archives of Medical Research*, 31(6):539 – 545, 2000.

[35] E.H Rogers. Stability and convergence of approximation schemes. *Journal of Mathematical Analysis and Applications*, 20(3):442 – 453, 1967.

[36] Sara E Rosenbaum. *Basic pharmacokinetics and pharmacodynamics: An integrated textbook and computer simulations*. John Wiley & Sons, 2011.

[37] S Ruiz, JM Conil, B Georges, F Ravat, T Seguin, P Letocart, O Fourcade, and S Saivin. Ceftazidime dosage regimen recommendations in burn patients based on a monolix population pharmacokinetic study. *Critical Care*, 16(1):1–189, 2012.

[38] J.M. Sanz-Serna and M.N. Spijker. Regions of stability, equivalence theorems and the Courant-Friedrichs-Lewy condition. *Numerische Mathematik*, 49(2-3):319–329, 1986.

[39] Radojka M. Savic, France Mentré, and Marc Lavielle. Implementation and evaluation of the SAEM algorithm for longitudinal ordered categorical data with an illustration in pharmacokinetics-pharmacodynamics. *The AAPS Journal*, 13(1):44–53, 2011.

[40] L. F. Shampine, I. Gladwell, and S. Thompson. *Solving ODEs with MATLAB*. Cambridge University Press, 2003.

[41] L.F. Shampine and S. Thompson. Solving DDEs in matlab. *Applied Numerical Mathematics*, 37(4):441 – 458, 2001.

[42] A. M. Smith, J. A. McCullers, and F. R. Adler. Mathematical model of a three-stage innate immune response to a pneumococcal lung infection. *Journal of Theoretical Biology.*, 276:106–116, 2011.

[43] M. Sofroniou and G. Spaletta. Construction of explicit Runge-Kutta pairs with stiffness detection. *Mathematical and Computer Modelling*, 40(11-12):1157 – 1169, 2004.

[44] J Srividhya, MS Gopinathan, and Santiago Schnell. The effects of time delays in a phosphorylation–dephosphorylation pathway. *Biophysical chemistry*, 125(2):286–297, 2007.

[45] Ch. Tsitouras. Runge-Kutta interpolants for high precision computations. *Numerical Algorithms*, 44(3):291–307, 2007.

[46] Ch. Tsitouras, I.Th. Famelis, and T.E. Simos. On modified Runge-Kutta trees and methods. *Computers & Mathematics with Applications*, 62(4):2101 – 2111, 2011.

[47] P. van der Houwen and B. Sommeijer. Explicit Runge-Kutta (-Nyström) methods with reduced phase errors for computing oscillating solutions. *SIAM Journal on Numerical Analysis*, 24(3):595–617, 1987.

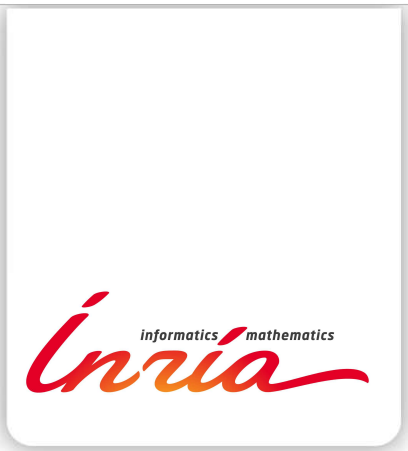

RESEARCH CENTRE
SACLAY – ÎLE-DE-FRANCE

1 rue Honoré d'Estienne d'Orves
Bâtiment Alan Turing
Campus de l'École Polytechnique
91120 Palaiseau

Publisher
Inria
Domaine de Voluceau - Rocquencourt
BP 105 - 78153 Le Chesnay Cedex
inria.fr

ISSN 0249-6399